Layered Materials

International Edition: DOI: 10.1002/anie.201411137
German Edition: DOI: 10.1002/ange.201411137

Encapsulation of Functional Organic Compounds in Nanoglass for Optically Anisotropic Coatings**

*Matthias Stöter, Bernhard Biersack, Sabine Rosenfeldt, Markus J. Leitl, Hussein Kalo, Rainer Schobert, Hartmut Yersin, Geoffrey A. Ozin, Stephan Förster, and Josef Breu**

Abstract: *A novel approach is presented for the encapsulation of organic functional molecules between two sheets of 1 nm thin silicate layers, which like glass are transparent and chemically stable. An ordered heterostructure with organic interlayers strictly alternating with osmotically swelling sodium interlayers can be spontaneously delaminated into double stacks with the organic interlayers sandwiched between two silicate layers. The double stacks show high aspect ratios of >1000 (typical lateral extension 5000 nm, thickness 4.5 nm). This newly developed technique can be used to mask hydrophobic functional molecules and render them completely dispersible in water. The combination of the structural anisotropy of the silicate layers and a preferred orientation of molecules confined in the interlayer space allows polymer nanocomposite films to be cast with a well-defined orientation of the encapsulated molecules, thus rendering the optical properties of the nanocoatings anisotropic.*

The industrial application of many functional organic molecules is often hampered by thermal and/or oxidative instability. Frequently, their processability may also be hampered by limited water solubility, while the masking and targeting of biologically active compounds is sought for many pharmaceuticals.[1]

[*] M. Stöter, Dr. H. Kalo, Prof. Dr. J. Breu
Lehrstuhl für Anorganische Chemie I, Universität Bayreuth
Universitätsstrasse 30, 95440 Bayreuth (Germany)
E-mail: Josef.Breu@uni-bayreuth.de
Dr. B. Biersack, Prof. Dr. R. Schobert
Organische Chemie I, Universität Bayreuth
Universitätsstrasse 30, 95440 Bayreuth (Germany)
Dr. S. Rosenfeldt, Prof. Dr. S. Förster
Physikalische Chemie I, Universität Bayreuth
Universitätsstrasse 30, 95440 Bayreuth (Germany)
M. J. Leitl, Prof. Dr. H. Yersin
Lehrstuhl für Physikalische Chemie, Universität Regensburg
Universitätsstrasse 31, 93053 Regensburg (Germany)
Prof. G. A. Ozin
Department of Chemistry, University of Toronto
80, St George Street, Toronto, M5S 3H6 (Canada)

[**] This work was financially supported by the Deutsche Forschungsgemeinschaft (SFB 840). We thank Prof. A. Fery, Physikalische Chemie II, University of Bayreuth, for making AFM equipment available. G.A.O. is the Government of Canada Research Chair in Materials Chemistry and Nanochemistry. He is deeply grateful to the Natural Sciences and Engineering Research Council of Canada for strong and sustained support of his work.

Supporting information for this article (including Experimental Details) is available on the WWW under http://dx.doi.org/10.1002/anie.201411137.

It is well-known in the case of various clathrates that encapsulation is capable of stabilizing even highly reactive species, such as of S_3^- ions in ultramarine. Moreover, intercalation results in the functional species no longer being in direct contact with the solvent. Instead, the dispersability is determined by the surface properties of the hybrid material. A large surface potential, for example, allows for robust electrostatic stabilization of aqueous suspensions.[2]

A layered host may offer the additional advantage of pronounced inherent structural anisotropy. Consequently, the interlayer structure formed by the intercalation of organic compounds between a sandwich of two layers ensures a well-defined orientation in the confined space.[3,4] Such a controlled arrangement of molecules is of key importance for efficient light absorption in organic solar cells and for spintronics.[5,6] In this regard, Kunz et al. have shown that the intercalation of $[Ru(bpy)_3]^{2+}$ (bpy = 2,2′-bipyridine) into a synthetic clay mineral leads to the polarized emission of light.[7]

Recently, we established a general synthetic procedure for the synthesis of ordered functional heterostructures, where interlayers with a functional molecular moiety strictly alternate with hydrated inorganic Na^+ interlayers.[8] Surprisingly, we now succeeded in spontaneously delaminating this material into double stacks of two highly transparent, flexible silicate layers that encapsulate a central organic layer of oriented functional molecules. Moreover, the large aspect ratio of these delaminated double stacks inevitably leads to perfectly textured films upon casting suspensions on flat substrates, which in turn results in a pseudoepitaxial orientation of the encapsulated functional moiety.

A melt-synthesized sodium hectorite ($[Na_{0.5}]^{inter}[Mg_{2.5}Li_{0.5}]^{oct}[Si_4]^{tet}O_{10}F_2$; Na-hec) can be synthesized with perfectly homogeneous charge density.[9] Any molecular interlayer cation that assembles into densely packed structures that show a charge density significantly higher or lower that of the layered silicate host allows for formation of ordered interstratified heterostructures.[8]

For example, intercalation of the fluorescent stilbazolium dye *N*-hexadecyl-4-(3,4,5-trimethoxystyryl)-pyridinium (subsequently shortened to dye) into well-characterized Na-hec[9] at a level whereby 38 % of the pristine interlayer cation (Na^+) is exchanged by dye leads to a perfectly ordered interstratified heterostructure[8] with strictly alternating layers of hydrated Na^+ and dye. The formation of the heterostructures is based on the partition equilibrium between the intercalated dye and the dye in solution. Although the dye will prefer the intercalated state and thus must have certain hydrophobicity, it still needs to show a reasonable solubility. Ethanol/water ratios of 4:1 were therefore used for the partial ion exchange.

For other dyes, the solubility needs to be adjusted. In the mixture used here, the swelling of the Na^+ interlayers is restricted to the two-layer hydrate and no exfoliation is observed at the stage where the heterostructure is formed.[8] Surprisingly, we now find that immersing the microcrystalline powder of the ordered interstratified heterostructure into deionized water results in the material swelling (Figure 1) into

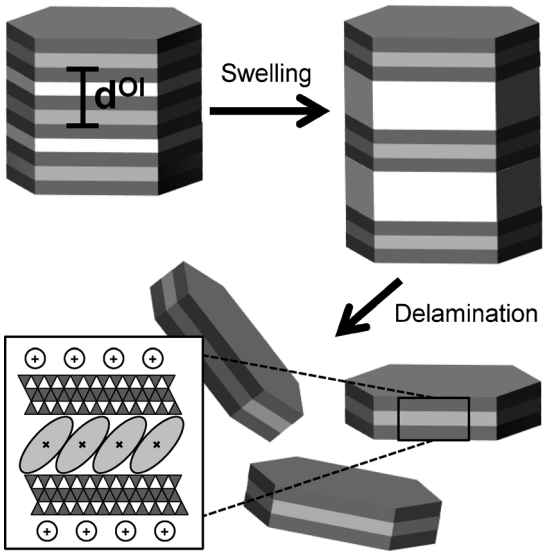

Figure 1. Delamination of the ordered interstratified heterostructured powder along swollen sodium interlayers (white) to produce water-dispersible double stacks with an oriented interlayer of encapsulated hydrophobic dye (gray).

a yellow gel with a high viscosity. A concomitant huge increase in sample volume (Figure S1) is observed, which indicates a delamination of the one-dimensional crystals into thinner nanoplatelets. Stable suspensions are formed at higher dilution, and a "Schlieren" texture implies a high stability of the suspension in water (Figure S2). Drying the diluted suspension on a flat substrate leads to a film that shows a good wettability for H_2O, comparable to the wettability of the pristine Na-hec. This finding suggests that the hydrophobic dye is not released upon swelling, but is irreversibly immobilized by intercalation (Figure S3). This is further supported by the high negative streaming potential of the double stacks that resembles the potential of the delaminated unmodified layered silicate, thus suggesting a similar surface charge.

Apparently, the hydration enthalpy of the Na^+ interlayers is still sufficient to trigger osmotic swelling, where the distance between individual platelets is determined simply by the silicate/water ratio. Upon swelling, the hydrophobic dye remains encapsulated between two 1 nm thick silicate layers. The diluted suspensions are transparent (Figure S4, right). The scattering of green laser light and a strong and homogeneous fluorescence under UV irradiation at 366 nm demonstrate that the double stacks are highly dispersed with the fluorescent dye molecules sandwiched between the silicate layers (Figure S4, left).

Final proof of the existence of double stacks comes from small-angle X-ray scattering (SAXS) studies. The SAXS pattern of the ordered interstratified heterostructured powder scales in the low q range ($q < 0.7\ nm^{-1}$) according to q^{-4}, which is typical for bulk 3D objects such as crystals, and confirms the mesoscopic length scale of the one-dimensional crystalline stacks (Figure 2d). The scaling of q for the most

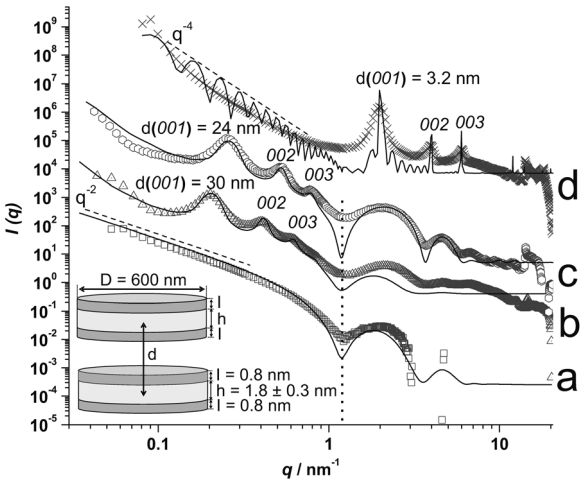

Figure 2. Experimental SAXS patterns (symbols) for aqueous suspensions of a) 2.5 wt% (square), b) 15 wt% (triangle), c) 20 wt% (hexagon), and d) the pristine ordered interstratified heterostructured powder (cross). The continuous lines correspond to calculated intensities based on a model of stacked "hamburgers" (see the Supporting Information for further details). The dotted line represents the position of the first minimum of the form factor, which is correlated to the thickness of one "hamburger" ($h+2l$). The scaling of q is indicated by dashed lines (only shown for the 2.5 wt% suspension and the ordered interstratified heterostructured powder).

diluted (2.5 wt%) suspension, however, changes to q^{-2}, which is typically observed for platelet-like objects (Figure 2a). The change in the scaling indicates a huge increase in aspect ratio, most probably because of delamination into thinner nanoplatelets upon swelling. This is further supported by a continuous shift of the average distance between double stacks (d) to lower q values as the water content is increased. The d spacing increases from 3.2 nm in the dry powder to 24 nm at 20 wt% and finally to 30 nm at 15 wt% suspension. The disappearance of the *00l* series for the most diluted 2.5 wt% suspension indicates a loss of positional correlation in the 2D SAXS pattern (Figures S5 and S6). At this stage, the material is swollen to a degree where the double stacks are separated far enough (> 60 nm) to realize an apparently isotropic orientation of the platelets. It is noteworthy that the intensity minima of the form factor oscillation at $q = 1.2\ nm^{-1}$ is the same for all suspensions of various concentrations. This value corresponds to a platelet thickness of 3.4 nm, which again corroborates the delamination into double stacks. The formation of individual double stacks was further verified by atomic force microscopy (AFM) of samples obtained from a highly diluted delaminated suspension. AFM confirms double stacks with a height of 4.5 nm (Figure 3), a value corresponding to the sum of the heights of two hydrated

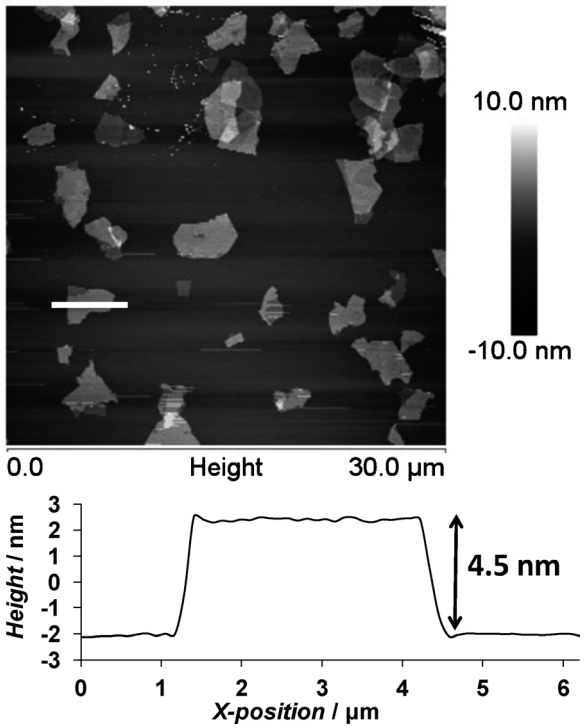

Figure 3. AFM image of a diluted aqueous suspension (0.01 mg mL^{-1}) dried on a silicon wafer illustrating the presence of double stacks with a height of 4.5 nm. The height profile of a platelet (white bar) is included.

silicate layers with a monolayer of dye encapsulated in between. The van der Waals thickness of one silicate layer is 0.96 nm.[9] The thickness of the dye interlayer can be deduced from a powder X-ray diffractogram (PXRD) recorded on a film of restacked double stacks dried at 0% relative humidity (r.h.; Figure S7) to be approximately 1.6 nm (3.52 nm−2 × 0.96 nm). It is noteworthy that the AFM measurement is performed under ambient conditions at approximately 50% r.h. Consequently, the Na^+ ions on both surfaces of the double stack are expected to be octahedrally coordinated by water (0.54 nm[10] on each side), summing to a total height of the double stack of 4.6 nm (2 × 0.96 nm + 1.6 nm + 2 × 0.54 nm).

Encapsulation of the hydrophobic dye between two silicate layers not only allows its dispersion in water but also significantly influences the solid-state optical properties of the fluorophore. Compared to the bromide salt of the dye, the intercalated dye no longer shows the additional absorption and emission bands at higher wavelengths (Figures S8 and S9), which are usually attributed to J-type dimers.[4] While such a change in structure might be expected as a consequence of the confinement between the layers, the increase in the emission quantum yield is somewhat surprising. The dye bromide salt shows a photoluminescence quantum yield (QY) of 3%, while the QY for the crystalline ordered interstratified heterostructured powder and the delaminated double stacks increases to 11% and 7%, respectively. Comparable improvement of the QY was obtained for a similar stilbazolium compound after microencapsulation in micelles, where torsional motions and nonradiative relaxation from the excited to the ground state are reduced.[11] Indeed, the confinement between the silicate layers might well impose restrictions on changes in the geometry of the luminescent molecule upon a transition between these states. These restrictions might be responsible for the increased QY observed.

When casting films of the delaminated suspension, the huge aspect ratio of double stacks of > 1000 (typical diameter 5000 nm, thickness 4.5 nm, Figure 3) will inevitably produce texture, as already indicated by the well-defined *00l* series observed by PXRD (Figure S7). Additionally, 2D SAXS measurements of the films were performed to judge the quality of the platelet texture (Figure 4).

In the transmission geometry, only a continuous ring of the *hk* band is visible, which is caused by a random, statistically isotropic orientational distribution of restacked double stacks within the film plane (Figure 4, top, and Figure S10). In the parallel geometry, mainly one *00l* series running along a fixed reciprocal direction can be observed, which indicates

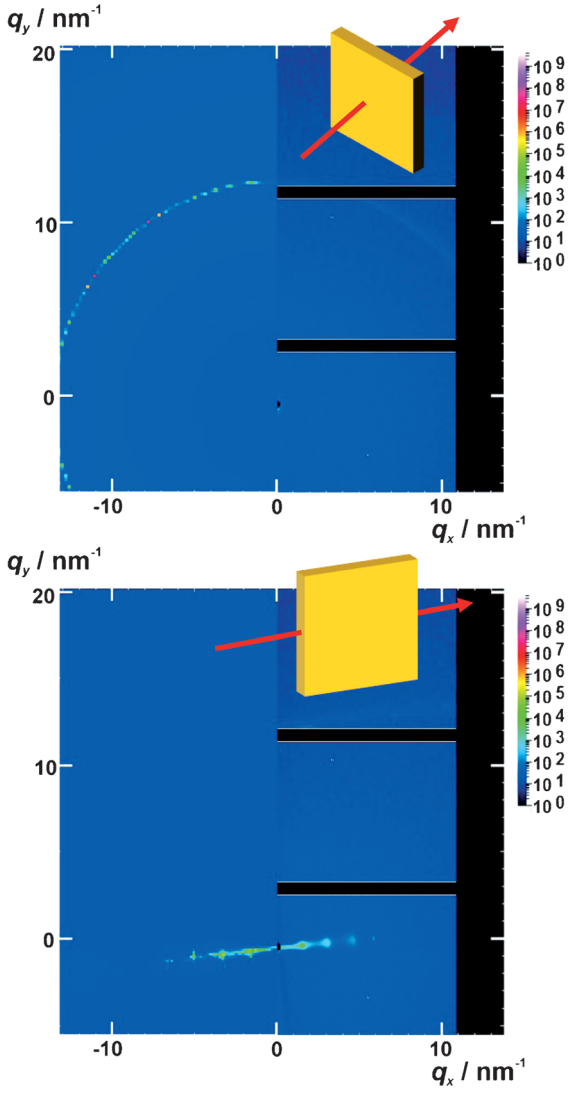

Figure 4. Measured (right) and calculated (left) 2-dimensional SAXS patterns of a textured film of delaminated and restacked double stacks in the transmission (top) and parallel geometry (bottom).

an anisotropic (textured) stacking of the double stacks orthogonally to the film plane (Figure 4, bottom, and Figure S10). From the coherence length in the azimuthal direction and the *d* spacing, an angle derivation of about 2° is found, which indicates a nearly perfect texture (see the Supporting Information for details).

The double stacks can be easily compounded into any polymer matrices of choice. The external Na^+ ions might have to be replaced by appropriate organic cations in the case of more hydrophobic matrices. As a proof of principle, we produced nanocomposite films with 50 wt% inorganic content by solution-casting delaminated double stacks mixed with an aqueous solution of polyvinyl alcohol (PVOH). SAXS patterns confirmed a highly anisotropic structure, thus corroborating the efficient texturing also in polymer matrices (Figure S11). TEM and SEM images of a cross-section of the nanocomposite film illustrate the layered structure and the presence of double stacks (Figures S12 and S13). The good texture is also reflected by a significantly improved oxygen barrier. The transmission rate of the nanocomposite film is four times lower than the unfilled PVOH film (Table S1), which indicates that the encapsulated dye will be protected from oxygen attack. Thermal analysis, moreover, indicates that the thermal stability of the encapsulated dye is improved by as much as 100 °C compared to the dye bromide salt (Figure S14). The decomposition temperature of the nanocomposite increases by approximately 30 °C compared to the neat PVOH matrix (Figure S15).

As indicated by the changes in the UV spectra, and as recently shown for a bulk layered silicate crystal intercalated with $[Ru(bpy)_3]^{2+}$,[7] the surface corrugation of the layered silicate will orientate molecules when confined between silicate layers. Consequently, a well-textured film of delaminated and restacked double stacks is expected to feature optical anisotropy with respect to absorption and emission of linearly polarized light.[4,12]

x- and *y*-polarized UV/Vis spectra of the textured film of delaminated and restacked double stacks and the nanocomposite film are shown in Figure 5 and Figure S17, respectively. The *y*-polarized UV/Vis spectra do not change as the δ angle increases, thus indicating a statistically isotropic orientation of the transition moments within the film surface, as a result of a random orientation within the *xy* plane. However, the *x*-polarized UV/Vis spectra show a linear reduction of the absorption as the δ angle increases, thus indicating optical anisotropy (see Figure S18 and the Supporting Information for more details) because of a fixed orientation of the transition moments along the *z* direction. Similar results were obtained for the nanocomposite film (Figure S19).

In conclusion, a general strategy is reported for the synthesis of nanosized layered hybrid materials where a functional organic cation is encapsulated between two transparent 1 nm thin silicate layers. Encapsulation assists dispersion of hydrophobic organic compounds in water, which bodes well for their use in medical applications such as photodynamic therapy and drug delivery. Additionally, the structural anisotropy of the clay mineral host in combination with the preferred orientation of the guest facilitates the production of

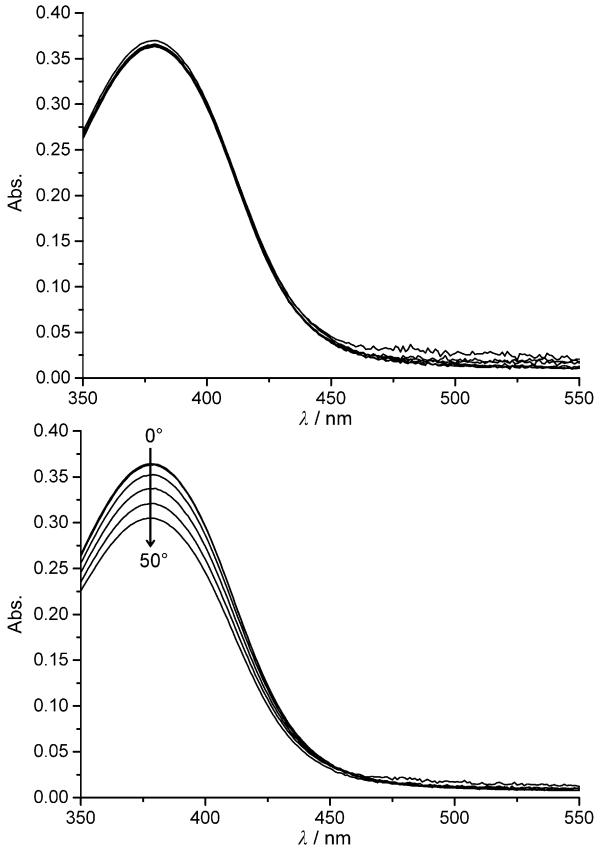

Figure 5. Corrected *y*- (top) and *x*-polarized (bottom) absorption spectra of a textured film of delaminated and then restacked double stacks. Both sets of spectra were obtained at different δ angles by turning the textured film around its *y* axis in 10° steps (arrow). The observed *x* polarization indicates orientation of the dye monolayer.

(polymer-based) nanocoatings with anisotropic physical properties. The concept should be transferable to other charged swelling inorganic layered materials, such as titanates[13] and niobates,[14] as long as an absolutely homogeneous charge density is warranted, which is essential to form ordered interstratifications.

Keywords: delamination · encapsulation · host compounds · layered materials · organic-inorganic hybrid composites

How to cite: *Angew. Chem. Int. Ed.* **2015**, *54*, 4963–4967
Angew. Chem. **2015**, *127*, 5047–5051

[1] Y. Chen, H. R. Chen, J. L. Shi, *Adv. Mater.* **2013**, *25*, 3144–3176.
[2] L. Li, L. Harnau, S. Rosenfeldt, M. Ballauff, *Phys. Rev. E* **2005**, *72*, 051504.
[3] S. Takagi, T. Shimada, Y. Ishida, T. Fujimura, D. Masui, H. Tachibana, M. Eguchi, H. Inoue, *Langmuir* **2013**, *29*, 2108–2119.
[4] V. Martínez Martínez, F. L. Arbeloa, J. B. Prieto, I. L. Arbeloa, *Chem. Mater.* **2005**, *17*, 4134–4141.
[5] O. Guskova, C. Schünemann, K. J. Eichhorn, K. Walzer, M. Levichkova, S. Grundmann, J. U. Sommer, *J. Phys. Chem. C* **2013**, *117*, 17285–17293.
[6] M. A. Niño, I. A. Kowalik, F. J. Luque, D. Arvanitis, R. Miranda, J. J. de Miguel, *Adv. Mater.* **2014**, *26*, 7474–7479.

[7] D. A. Kunz, M. J. Leitl, L. Schade, J. Schmid, B. Bojer, U. T. Schwarz, G. A. Ozin, H. Yersin, J. Breu, *Small* **2015**, *11*, 792 – 796.
[8] M. Stöter, B. Biersack, N. Reimer, M. Herling, N. Stock, R. Schobert, J. Breu, *Chem. Mater.* **2014**, *26*, 5412 – 5419.
[9] M. Stöter, D. A. Kunz, M. Schmidt, D. Hirsemann, H. Kalo, B. Putz, J. Senker, J. Breu, *Langmuir* **2013**, *29*, 1280 – 1285.
[10] H. Kalo, W. Milius, J. Breu, *RSC Adv.* **2012**, *2*, 8452 – 8459.
[11] L. F. M. Ismail, *J. Lumin.* **2012**, *132*, 2512 – 2520.
[12] V. Martínez, S. Salleres, J. Banuelos, F. L. Arbeloa, *J. Fluoresc.* **2006**, *16*, 233 – 240.
[13] F. Geng, R. Ma, A. Nakamura, K. Akatsuka, Y. Ebina, Y. Yamauchi, N. Miyamoto, Y. Tateyama, T. Sasaki, *Nat. Commun.* **2013**, *4*, 1632.
[14] M. M. Fang, C. H. Kim, G. B. Saupe, H. N. Kim, C. C. Waraksa, T. Miwa, A. Fujishima, T. E. Mallouk, *Chem. Mater.* **1999**, *11*, 1526 – 1532.

Received: November 17, 2014
Published online: February 20, 2015

